
ANALYTICAL DESCRIPTION OF THE TIME-OVER-THRESHOLD METHOD BASED ON THE TIME PROPERTIES OF PLASTIC SCINTILLATORS EQUIPPED WITH SILICON PHOTOMULTIPLIERS

N. Karpushkin, D. Finogeev, F. Guber, D. Lyapin, A. Makhnev, S. Morozov, D. Serebryakov

Institute for Nuclear Research of the Russian Academy of Sciences
60-letiya Oktyabrya prospekt 7a, Moscow 117312, Russia
karpushkin@inr.ru

ABSTRACT

A new high-granular compact time-of-flight neutron detector for the identification and energy measurement of neutrons produced in nucleus-nucleus interactions at the BM@N experiment, Dubna, Russia, at energies up to 4 AGeV is under development. The detector consists of approximately 2000 fast plastic scintillators, each with dimensions of $40 \times 40 \times 25$ mm³, equipped with SiPM (Silicon Photomultiplier) with an active area of 6×6 mm². The signal readout from these scintillators will employ a single-threshold multichannel Time-to-Digital Converter (TDC) to measure their response time and amplitude using the time-over-threshold (ToT) method. This article focuses on the analytical description of the signals from the plastic scintillator detectors equipped with silicon photomultipliers. This description is crucial for establishing the ToT-amplitude relationship and implementing slewing correction techniques to improve the time resolution of the detector. The methodology presented in this paper demonstrates that a time resolution at the 70 ps level can be achieved for the fast plastic scintillator coupled with silicon photomultiplier with epitaxial quenching resistors.

1 Introduction

The equation of state (EoS) of nuclear matter establishes the relationship between pressure, density, energy, and temperature, and incorporates the symmetry energy term that characterizes the isospin asymmetry of nuclear matter. Previous studies have extracted EoS information from isospin-symmetric heavy-ion collision experiments, particularly by analyzing the azimuthal distributions of protons in Au + Au collisions at beam energies up to 1.5A GeV at GSI [1] and at BNL with beam energies ranging from 2 to 8 AGeV [2]. However, to gain further insights into the EoS of isospin-symmetric nuclear matter, it is essential to explore the azimuthal asymmetry of neutrons produced in high-density nuclear matter in heavy-ion collisions. Understanding the EoS is crucial for studying astrophysical phenomena like neutron stars and their mergers.

The BM@N experiment at NICA, JINR, Dubna, Russia [3, 4, 5], aims to investigate nuclear matter properties at baryon densities of 2-4 ρ_0 , created in heavy-ion collisions with beam energies up to 4 AGeV. To measure neutron yields and azimuthal flows, providing valuable information about the contribution of the symmetry energy term to the equation of state of dense nuclear matter, a high granular neutron detector with a large number of readout channels is currently in development [6].

The proposed detector will utilize fast plastic scintillators with dimensions of $40 \times 40 \times 25$ mm³. JINR-produced scintillator based on polystyrene with additions of 1.5% paraterphenyl and 0.01% POPOP is considered as main option. The use of more fast scintillators, such as EJ-230 [7], are considered also. For scintillation signal detection, new fast silicon photomultipliers with epitaxial quenching resistors (SiPM EQR15 11-6060D-S) [8] with a size of 6×6 mm² will be employed.

Given that the detector will have multiple readout channels (~ 2000), the new TDC (Time-to-Digital Converter) board with a 100 ps bin width is now under development [9]. Each readout channel will connect to a comparator operating

at a constant threshold. The detector will record the response time, enabling the determination of a particle's time-of-flight and subsequent kinetic energy calculation. The signal amplitude will be indirectly measured by analyzing the time-over-threshold (ToT). For the calibration of the multichannel detector, short-pulsed LEDs (Light-Emitting Diode) will be used.

In this paper, we propose an analytical model description for an exponentially decaying light flash registered by a SiPM. The analytical model allows us to parametrise the leading and trailing edges times at constant threshold. This approach enables us to introduce appropriate corrections to improve the time resolution. Another purpose of constructing an analytical description of signals based on physical principles is to convert calibration constants obtained using a laser (or LED) for scintillation signals.

2 Analysis of the signals shape from fast plastic scintillator and silicon photomultiplier

2.1 Processes inside the SiPM

The SiPM (Silicon Photomultiplier) comprises an array of SPAD (Single Photon Avalanche Diode) – pixels. These pixels are maintained in a "ready" quasi-stable state through the application of bias voltage, transitioning them into the Geiger mode. Upon absorption of a photon, an avalanche process is initiated within the corresponding pixel, leading to a rapid rise in current to its maximum value. The avalanche is subsequently quenched to ensure stable operation. In case of passive quenching this is accomplished through the incorporation of a quenching resistor. Classic SiPMs utilize polysilicon quenching resistors located on the device's surface, while one of the current development directions is focused on SiPMs with epitaxial quenching resistors [10]. In such SiPMs, the quenching resistance is integrated within the epitaxial layer, increasing the density of cells. Reduced junction capacitance combined with a relatively low quenching resistance, leads to a fast recovery time. Additionally, the high geometric fill factor of these SiPMs allows for a wide dynamic range with high photon detection efficiency (PDE).

A comprehensive analysis of the processes in a SiPM, including consideration of all parasitic processes, can be found in the detailed study [11], while the pulse shape discussion is available in [12, 13, 14]. In this article, we restrict ourselves to an approximate description, which, however, will allow us to reflect the essence observed in the experiment: we will characterize the impulse response function of the SiPM by the characteristic time $R_s C_T$, where R_s stands for the sum of load resistance and low intrinsic SiPM resistance, and C_T is the total SiPM capacitance.

2.2 Characterizing Time Response in Plastic Scintillator Readout with SiPMs

When charged particles traverse through a plastic scintillator, a flash of light is emitted, providing a measurable signal with initial number of photons N_{ph}^0 . The rise time τ_R and decay time τ_D of the scintillation flash define its time characteristics. Notably, the rise time is typically negligible, allowing its omission in subsequent analyses.

$$N_{ph}(t) = N_{ph}^0 (1 - e^{-t/\tau_R}) e^{-t/\tau_D} \approx N_{ph}^0 e^{-t/\tau_D}. \quad (1)$$

Onwards we consider a general form of an exponentially decaying light signal with decay time τ_{in} in the form $N_{ph}(t) = N_{ph}^0 e^{-t/\tau_{in}}$, illuminating silicon photomultiplier.

This allows us to express the voltage across the load resistance when a light flash illuminates the SiPM. This voltage can be obtained as a product of the load resistance and the convolution of the photoelectron current, denoted as $f(t) = I_{p.e.} = \eta e \frac{dN_{ph}}{dt}$, with the impulse response function of the SiPM, denoted as $g(t) = \frac{1}{R_s C_T} e^{-t/R_s C_T}$. In this notation, η represents the photon detection efficiency (PDE), e represents the charge of an electron. The impulse response function is normalized to unity. We omitted the discharge phase component in our analysis due to its relatively short characteristic time.

$$V(t) = R_s (f * g)(t) = -\frac{\eta e N_{ph}^0}{C_T \tau_{in}} \int_0^t e^{-\frac{x}{\tau_{in}}} e^{-\frac{t-x}{R_s C_T}} dx = \frac{\eta e N_{ph}^0 R_s}{R_s C_T - \tau_{in}} \left(e^{-t/R_s C_T} - e^{-t/\tau_{in}} \right). \quad (2)$$

A similar solution can be obtained from the differential equation if we consider the SiPM "integrally". We will say that the current through the SiPM is determined by two simultaneous processes: the discharging photoelectron current and the recharge current. The recharge current is determined at each moment of time only by the value of the charge q stored in the SiPM.

$$\frac{dq}{dt} = I_{p.e.} + I_{recharge} \quad V_{bias} - R_s I_{recharge} = \frac{q}{C_T}. \quad (3)$$

Solving such a differential equation with the initial condition $q(0) = C_T V_{bias}$, we obtain an expression for the voltage across the load resistor:

$$V(t) = R_s I_{recharge} = \frac{\eta e N_{ph}^0 R_s}{R_s C_T - \tau_{in}} \left(e^{-t/R_s C_T} - e^{-t/\tau_{in}} \right). \quad (4)$$

2.3 Addressing Derivative Discontinuity

The solution for the voltage across the load resistance (Equations 2, 4) exhibits a derivative discontinuity at zero. Additionally, experimental data shows a slight difference in the amplitudes of the two terms. To address this, we introduce a phase shift to the fast exponent by a value $\tau_{in} \ln(1 - p)$. As a result, the fast component, responsible for the input signal, will lead the component related to recharge. To achieve smoother behavior at the beginning of the signal, the conditions of this solution are matched with a parabolic solution at zero. This parametrization is also based on experimental data. With such a phase shift, at time 0, the signal reaches a certain constant fraction of its amplitude.

$$V_0 = \frac{\eta e N_{ph}^0 R_s}{R_s C_T - \tau_{in}} \quad T_p = \frac{2p\tau_{in} R_s C_T}{(1 - p)R_s C_T - \tau_{in}}$$

$$V(t) = \begin{cases} pV_0 \left(\frac{t}{T_p} + 1 \right)^2 & \text{if } -T_p < t < 0 \\ V_0 \left(e^{-\frac{t}{R_s C_T}} - (1 - p)e^{-\frac{t}{\tau_{in}}} \right) & \text{if } t \geq 0 \end{cases} \quad (5)$$

3 Comparison of Model with Experimental Data

Parametrization given in Equation 5 is used to reproduce the signal from a picosecond laser, detected by the SiPM EQR15 11-6060D-S [8] with a load resistor $R_l = 33\Omega$ and is shown in the left side of Figure 1. The grey area represents multiple waveforms that are superimposed and normalized to present the characteristic data curve. The red line corresponds to a model (Equation 5) with characteristic time parameters obtained from spectral analysis using the Prony Least Squares method [15]. The light grey area represents multiple superimposed waveforms obtained from the common-base amplifier giving a low input impedance of less than 10Ω . This amplifier has narrower bandwidth compared to the one used in previous measurements, resulting in a longer rise time. Such a data curve cannot be described using the simplified analytical model compiled and is provided here solely for illustrative purposes.

A signal from fast laser flash passing through the measuring circuit broadens to a characteristic time of $\tau_{in} = 1.6 \pm 0.2$ ns. The theoretical characteristic recharge time, determined by a load resistance $R_l = 33\Omega$ and a SiPM capacitance $C_T \approx 200pF$ [8], is approximately 6.7 ns. However, in the data, the observed time is 8.8 ± 0.8 ns (as shown in Figure 1 on the right), which suggests the presence of low additional intrinsic resistance in the SiPM. The amplitudes of the exponential components exhibit a linear correlation, and the slope of this correlation indicates that the value of p in this case is approximately 0.3. These parameters must be determined by a spectral analysis for each detector arrangement. The characteristic decay time parameters for fast JINR-produced scintillator and EJ-230 scintillator are 3.9 ± 0.7 ns and 2.8 ± 0.5 ns respectively.

Furthermore, starting from a certain point, there is a discrepancy between the simplified theoretical parametrization (Equation 5) and the real data. Although we expect this discrepancy to have minimal impact, it should be considered in future analyses. This discrepancy is caused by a low-amplitude component with a large decay time ($\gg 1\mu s$) and can be addressed by a more accurate SiPM response parametrization.

4 Slewing correction and ToT method

As mentioned earlier, the neutron detector in the BM@N experiment will utilize a multichannel TDC for data collection to reduce the complexity and cost of readout electronics. The key information to extract from the data is the response time, as it determines the particle's time-of-flight and enables the calculation of its kinetic energy. However, when measuring time, a known issue arises regarding the dependency of the threshold crossing time on the signal

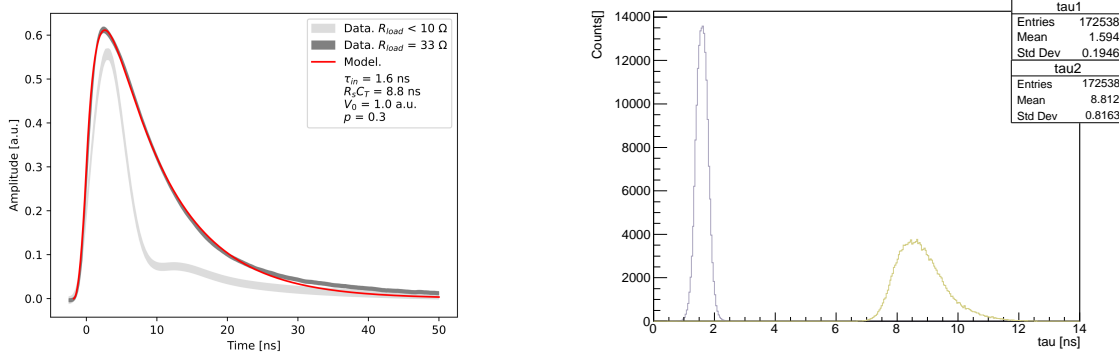


Figure 1: Left: Comparison between the SiPM measured data curve and model parametrisation. Right: distributions of the characteristic times of the parametrisation.

amplitude, commonly referred to as time walk or slewing. To address slewing, it is necessary to determine the signal amplitude, which will be indirectly achieved by measuring the ToT. Given the known waveform parameterization, straightforward calculations yield the following expressions for identifying the times at which the signal crosses the threshold θ [mV]:

$$t_1 = T_p \left(\sqrt{\frac{\theta}{pV_0}} - 1 \right) \quad t_2 = R_s C_T (\ln V_0 - \ln \theta) \quad (6)$$

To address slewing (time walk) correction, we can approximate it by calculating the ToT:

$$\text{slewing} \approx \frac{T_p}{\sqrt{p}} e^{-\frac{\text{ToT}}{2R_s C_T}} \quad (7)$$

Figure 2 shows the correlation between the arrival time of the signal and its ToT. The red line represents a parametrization given by Equation 7 with free parameters.

5 Characterization of Scintillator Light Signals and Time Resolution

The time resolution of the JINR-produced scintillator sample with dimensions of $40 \times 40 \times 25$ mm³ equipped with the SiPM EQR15 11-6060D-S, was measured using a 280-MeV electron beam at the "Pakhra" synchrotron at LPI [16]. For comparison, the time resolution was also measured for a sample from the EJ-230 scintillator with the same SiPM.

The time resolution of the scintillator samples was determined relative to the fast Cherenkov counter based on XP85012-FIT/Q microchannel photomultiplier tube signal, which has an estimated intrinsic time resolution of 22 ps [17]. The correction for slewing was applied using Equation 6, resulting in an improvement of the time resolution by approximately 50%. The achieved time resolution for laser light source, JINR-produced scintillator and EJ-230 scintillator are 45 ± 0 ps, 117 ± 1 ps and 74 ± 1 ps, respectively.

6 ToT method Amplitude Resolution Estimation

In the experiment, information about the signal amplitude will be available indirectly through its relationship with the ToT. To estimate the amplitude resolution, including the systematic error of the method, the correlation between ToT and amplitude was utilized. Figure 3 displays this correlation for data acquired with a laser, illustrating the full dynamic range of the detector, which spans approximately 1-8 MIP (Minimum Ionizing Particle; 1 MIP corresponds to ~ 200 mV). The red line in the figure represents the parametrization of this dependence using Equation 6.

To obtain estimates of statistical and systematic errors, we scanned over narrow ToT bins and analyzed the width of the amplitude distribution in each segment, as well as the difference between the average value of the amplitude distribution and the analytical parameterization. For data acquired with a laser, the estimates of statistical and systematic

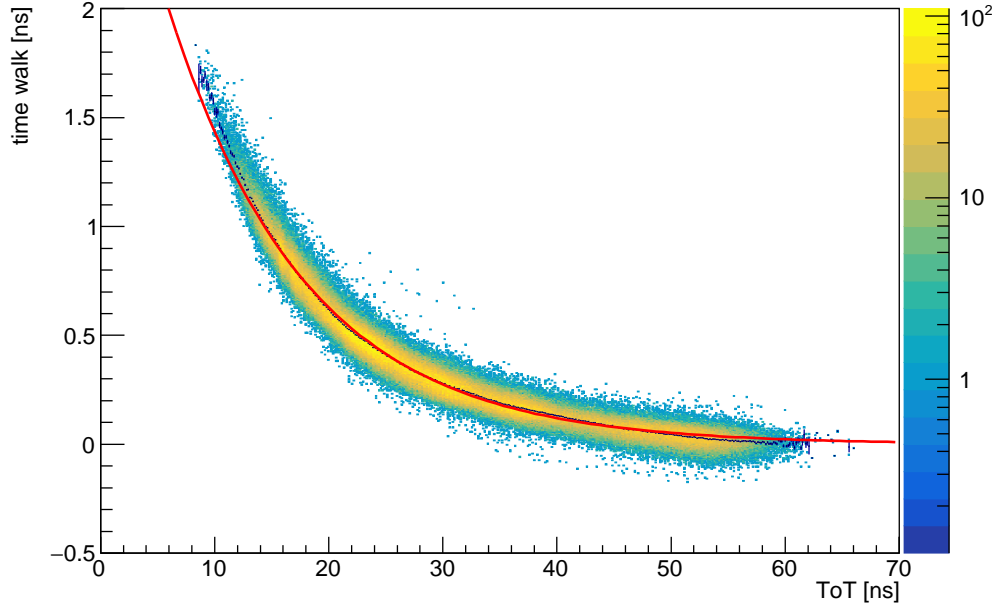


Figure 2: Time walk : ToT correlation. Data are taken from a SiPM EQR15 11-6060D-S illuminated by the picosecond laser. The red line represents the model given by Equation 7 with parameters $3.3e^{-ToT/12.1}$. The value $2R_sC_T = 12.1$ ns appears to be smaller than expected and is more in agreement with the SiPM datasheet value.

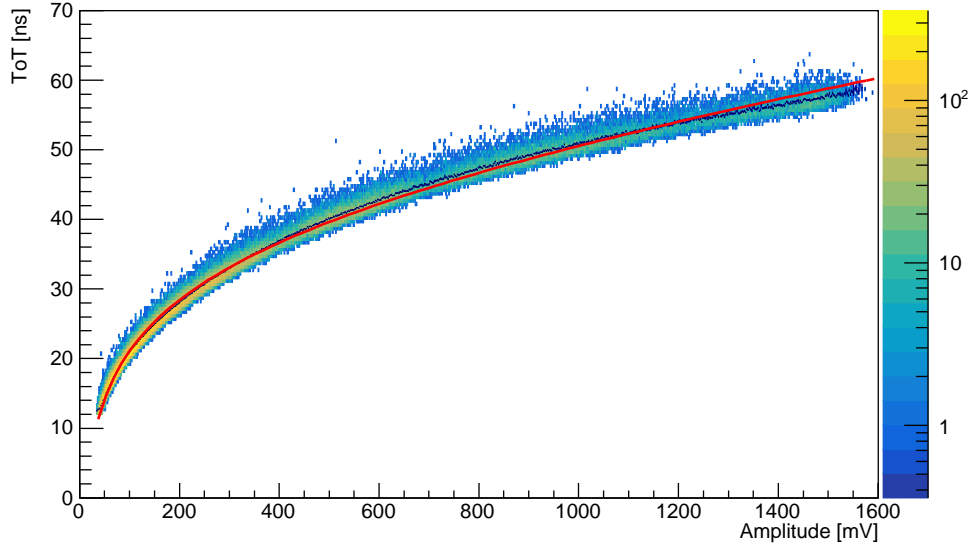


Figure 3: ToT : Amplitude correlation. Data were taken from a SiPM EQR15 11-6060D-S illuminated by the picosecond laser. The red line represents the model given by Equation 6.

errors are 8% and 5%, respectively. For the data collected using an electron beam, the values of statistical and systematic errors do not exceed 14% and 10%, respectively, for both tested scintillators. During these tests, a 1 cm thick lead bar was introduced into the electron beam to increase the possible spread of amplitudes.

7 Summary

The analytical description of the signals from fast scintillators with SiPM readout, with a primary focus on establishing the relationship between ToT and signal amplitude has been developed. The implementation of slewing correction techniques to improve the time resolution of the time-of-flight neutron detector, which is being developed for the BM@N experiment, has been demonstrated. The analytical description of signals based on timing properties of fast scintillators and SiPMs was developed allowing to convert calibration constants obtained using a laser (or LED) for scintillation signals. The detector employs fast plastic scintillators combined with silicon photomultipliers with epitaxial quenching resistors and features a multichannel TDC readout scheme. Through the methodology presented in this paper, the time resolution of approximately 130 ps is achieved for the $40 \times 40 \times 25$ mm³ scintillation detector based on JINR type of scintillator equipped with EQR15 11-6060D-S SiPM with active area 6×6 mm². The best time resolution of approximately 70 ps, has been obtained for the sample of EJ-230 scintillator and the same SiPM.

Acknowledgments

This work was carried out at the Institute for Nuclear Research, Russian Academy of Sciences, and supported by the Russian Scientific Foundation grant №22-12-00132.

References

- [1] A. Le Fèvre, Y. Leifels, W. Reisdorf, J. Aichelin, C. Hartnack, Constraining the nuclear matter equation of state around twice saturation density, Nucl. Phys. A 945 (2016) 112–133. arXiv:1501.05246, doi:10.1016/j.nuclphysa.2015.09.015.
- [2] C. Pinkenburg, et al., Elliptic flow: Transition from out-of-plane to in-plane emission in Au + Au collisions, Phys. Rev. Lett. 83 (1999) 1295–1298. arXiv:nucl-ex/9903010, doi:10.1103/PhysRevLett.83.1295.
- [3] Bm@n.
URL <https://bmn.jinr.ru>
- [4] M. Kapishin, Heavy Ion BM@N and MPD Experiments at NICA, JPS Conf. Proc. 32 (2020) 010093. doi:10.7566/JPSCP.32.010093.
- [5] P. Senger, The heavy-ion program at the upgraded Baryonic Matter@Nuclotron Experiment at NICA, PoS CPOD2021 (2022) 033. doi:10.22323/1.400.0033.
- [6] F. Guber, et al., Development of High Granular Neutron Time-of-Flight Detector for the BM@N experiment, to be updated. arXiv:0000.0000.
- [7] Eljen technology.
URL <https://eljentechnology.com/products/plastic-scintillators/ej-228-ej-230>
- [8] Novel device laboratory beijing, eqr15 series sipms.
URL <http://www.ndl-sipm.net/PDF/Datasheet-EQR15.pdf>
- [9] D. Finogeev, et al., Development of 100 ps TDC based on Kintex 7 FPGA for the High Granular Neutron Time-of-Flight detector for BM@N experiment, to be updated. arXiv:0000.0000.
- [10] T. Zhao, R. Preston, J. Jiang, J. Jia, Y. Liu, K. Liang, R. Yang, D. Han, Progresses of silicon photomultiplier technologies with epitaxial quenching resistors, Nuclear Instruments and Methods in Physics Research Section A: Accelerators, Spectrometers, Detectors and Associated Equipment 912 (2018) 252–254, new Developments In Photodetection 2017. doi:https://doi.org/10.1016/j.nima.2017.11.069.
URL <https://www.sciencedirect.com/science/article/pii/S0168900217313165>
- [11] S. Gundacker, A. Heering, The silicon photomultiplier: fundamentals and applications of a modern solid-state photon detector, Physics in Medicine & Biology 65 (17) (2020) 17TR01. doi:10.1088/1361-6560/ab7b2d.
URL <https://dx.doi.org/10.1088/1361-6560/ab7b2d>

- [12] F. Corsi, C. Marzocca, A. Perrotta, A. Dragone, M. Foresta, A. Del Guerra, S. Marcatili, G. Llosa, G. Collazuol, G.-F. Dalla Betta, N. Dinu, C. Piemonte, G. Pignatelli, G. Levi, Electrical characterization of silicon photomultiplier detectors for optimal front-end design, 2006, pp. 1276 – 1280. doi : 10.1109/NSSMIC.2006.356076.
- [13] G. Giustolisi, G. Palumbo, P. Finocchiaro, A. Pappalardo, A simple extraction procedure for determining the electrical parameters in silicon photomultipliers, 2013 European Conference on Circuit Theory and Design, ECCTD 2013 - Proceedings (2013) 1–4doi : 10.1109/ECCTD.2013.6662194.
- [14] A. Duara, J. Lapington, J. Williams, S. Leach, D. Ross, T. Rawlins, Experimental and extraction procedure for the electrical characterisation of silicon photomultiplier detectors, Nuclear Instruments and Methods in Physics Research Section A: Accelerators, Spectrometers, Detectors and Associated Equipment 979 (2020) 164483. doi : <https://doi.org/10.1016/j.nima.2020.164483>.
URL <https://www.sciencedirect.com/science/article/pii/S0168900220308809>
- [15] N. Karpushkin, F. Guber, A. Ivashkin, Application of the Prony least squares method for fitting signal waveforms measured by sam AIP Conference Proceedings 2163 (1) (2019) 030006. arXiv : <https://pubs.aip.org/aip/acp/article-pdf/doi/10.1063/1.5130092>.
doi : 10.1063/1.5130092.
URL <https://doi.org/10.1063/1.5130092>
- [16] S. Morozov, et al., Measurement of the time resolution of scintillation detectors with silicon photodetectors EQR-15 for the Time-of-Flight Neutron detector of the BM@N experiment, to be updated. arXiv : 0000.0000.
- [17] T. L. Karavicheva, on behalf of the ALICE Collaboration, The fast interaction trigger detector for the alice upgrade, Journal of Physics: Conference Series 798 (1) (2017) 012186. doi : 10.1088/1742-6596/798/1/012186.
URL <https://dx.doi.org/10.1088/1742-6596/798/1/012186>